Thermal entanglement of the spin-1/2 diamond chain

2012 J. Phys.: Conf. Ser. 343 012022

(http://iopscience.iop.org/1742-6596/343/1/012022)

Journal of Physics: Conference Series **343** (2012) 012022 doi:10.1088/1742-6596/343/1/012022

Thermal entanglement of the spin-1/2 diamond chain

L. Chakhmakhchyan[1,2], N. Ananikian[1], L. Ananikyan[1], and Č. Burdík[3]

[1] A.I. Alikhanyan National Science Laboratory, Alikhanian Br. 2, 0036 Yerevan, Armenia
[2] Institute for Physical Research, 0203 Ashtarak-2, Armenia
[3] Czech Technical University, Trojanova 13, 120 00 Prague 2, Czech Republic

E-mail: levonc@rambler.ru

Abstract. The entanglement thermal (equilibrium) properties in spin-1/2 Ising-Heisenberg model on an ideal diamond chain is analyzed. Due to the classical character of Ising-type exchange interactions between two neighboring antiferromagnetic Heisenberg dimers, the calculation of quantum entanglement (by tracing out Ising spins) can be performed for each of the dimers separately. The concurrence, as a measure of entanglement is obtained and different regimes depending on the values of exchange interactions are revealed. The effects of the magnetic field are incorporated and critical temperatures corresponding to the vanishing or arising of entanglement are considered.

1. Introduction

During the last two decades low-dimensional magnetic materials with competing interactions or geometrical frustration have become an intriguing research object due to a rich variety of unusual ground states and thermal properties as a result of zero and finite temperature phase transitions driven by quantum and thermal fluctuations respectively [1–5]. As fascinating models among these systems exhibiting interesting quantum phenomena, one should mention the ones having a diamond-chain structure consisting of diamond-shaped topological units along the chain (figure 1). The recent experimental results on the natural mineral azurite ($Cu_3(CO_3)_2(OH)_2$) [6] showed that Cu^{2+} ions of this material form a spin-1/2 diamond chain. Furthermore, the discovery of a plateau at 1/3 of the saturation value in the low-temperature magnetization curve [6] has triggered an intensive interest in the magnetic properties of azurite, both from theoretical and experimental points of view [7–10]. With all exchange constants being antiferromagnetic, azurite would fall into the class of geometrically frustrated magnets. However, despite the long-standing interest towards this natural mineral, there is still an open question concerning the strength and the type of exchange interactions in the compound. The first diamond spin chain was explored under a symmetrical condition $J_1 = J_3$ [11] that predicted magnetization plateaus both at 1/3 and 1/6 of saturation [12, 13]. Moreover, the frustrated diamond chain with ferromagnetic interactions $J_1, J_3 < 0$ and antiferromagnetic interaction $J_2 > 0$ was also investigated theoretically [14]. Namely, the controversy on these values seem to be cleared up only recently (the latest comparison of experimental and theoretical results can be found in Ref. [15]).

Motivated by the controversies presented above and the fact that different compounds can be described by means of a diamond chain , by a change in the values of coupling constants [16–18],

we shall explore the symmetrical spin-1/2 diamond chain with competing interactions J_1 and J_3 in a magnetic field. But, unfortunately, the rigorous theoretical treatment of geometrically frustrated quantum Heisenberg models is difficult to fulfil due to a non-commutability of spin operators involved in the Heisenberg Hamiltonian, which is also a primary cause of a presence of quantum fluctuations. Owing to this fact, we will use the recently proposed geometrically frustrated Ising-Heisenberg diamond chain model, depicted in figure 1 [19, 20].

In the present paper we will be mainly interested in the quantum entanglement properties of the spin-1/2 Ising-Heisenberg model on a generalized symmetrical diamond chain. It is well-known, that the entanglement is a generic feature of quantum correlations in systems that cannot be quantified classically [21, 22]. It provides a new perspective for understanding the quantum phase transitions (QPTs) and collective phenomena in many-body and condensed matter physics. This problem, which has been under scrutiny for nearly two decades, has recently attracted much attention [23–27]. A new line research points to a connection between the entanglement of a many-particle system and the existence of the QPTs and scaling [28, 29]. And afterwards a few experimental evidences have been reported for low-dimensional spin systems [30, 31], confirming the presence of entanglement in solid state materials.

If we return to the spin-1/2 Ising-Heisenberg model on a diamond chain and consider, that the nodal Ising spins represent a barrier for quantum fluctuations that are consequently restricted to elementary diamond-shaped units, then taking into account that each Heisenberg dimer interacts with its neighboring dimer through the Ising-type exchange, i.e. classical interaction, one finds the states of two adjacent dimers become separable (disentangled) [21, 22]. Thus, we can calculate concurrence (as a measure of pairwise entanglement [32, 33]), which characterizes quantum features of the system, for each dimer separately.

The rest of the paper is organized as follows: in section 2 we give a brief description of the spin-1/2 Ising-Heisenberg model on a generalized distorted diamond chain. The basic principles for calculation of concurrence as a measure of entanglement and phase structure of the ideal diamond chain ($J_1 = J_3$, $J_m = 0$) for both cases of a zero and non-zero magnetic field are discussed in section 3. Some comments and concluding remarks are drawn in section 4.

2. Spin-1/2 Ising-Heisenberg model on a generalized distorted diamond

We consider the general spin-$\frac{1}{2}$ Ising-Heisenberg model on a generalized distorted diamond chain (figure 1), which consists of monomeric and dimeric sites (empty and full circles in figure 1, respectively). Within the proposed Ising-Heisenberg model, the monomeric (nodal) sites are occupied by Ising spins, while the dimeric sites by Heisenberg-type spins. The Hamiltonian can be written as follows:

$$\mathcal{H} = \sum_{k=1}^{N} \mathcal{H}_k = \sum_{k=1}^{N} \Big[J_2 \mathbf{S}_{k_1} \mathbf{S}_{k_2} + \mu^z_{k_1}(J_3 S^z_{k_1} + J_1 S^z_{k_2}) + \mu^z_{k_2}(J_1 S^z_{k_1} + J_3 S^z_{k_2}) + J_m \mu^z_{k_1} \mu^z_{k_2} - H\left(S^z_{k_1} + S^z_{k_2} + \frac{\mu^z_{k_1} + \mu^z_{k_2}}{2} \right) \Big], \quad (1)$$

where the summations run over clusters (figure 1), $\mathcal{H}_k$ represents the Hamiltonian of the $k-th$ cluster, $\mathbf{S}_k = \{S^x_k, S^y_k, S^z_k\}$ denotes the Heisenberg spin-$\frac{1}{2}$ operator, μ_k is the Ising spin. Considering, that each Ising spin belongs simultaneously to two clusters, we have taken a 1/2 factor for Ising spins in the last term of (1), which incorporates the effects of external magnetic field. $J_i > 0$ $(i = 1, 2, 3, m)$ corresponds to the antiferromagnetic couplings. The system will be strongly frustrated due to the chain's geometry and existence of competing interactions $J_i's$ $(i = 1, 2, 3, m)$. The symmetrical diamond chain is obtained in the limit $J_1 = J_3$. When $J_1 = J_3$ and $J_m = 0$ we deal with the so called ideal diamond chain [19, 20]. In general case, when

$J_1 \neq J_3$ the symmetry of the chain is broken and one obtains the distorted diamond chain [15]. Before introducing the calculations and discussion we would like to emphasize the fact which was already discussed in section 1: the states of two neighboring Heisenberg dimers (with interaction J_2) are separable (disentangled), because of a classical character of the coupling between them (by means of the Ising spin). Hence we can calculate the entanglement for each of the dimers individually.

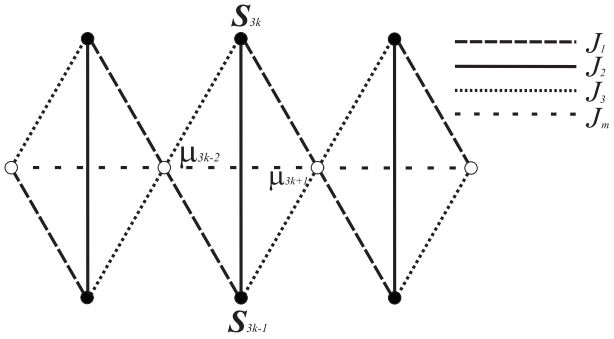

Figure 1. A cross-section of a generalized distorted diamond chain (k labels the number of the cluster). The empty (monomeric units) and full circles (dimeric units) denote lattice positions of the Heisenberg and Ising spins (within the proposed Ising-Heisenberg model), respectively. Solid lines schematically reproduce the Heisenberg J_2 interactions between dimeric units, while the broken ones label the Ising-type (nearest-neighbor J_1, J_3 and next-nearest neighbor J_m) interactions.

3. Concurrence and thermal entanglement of the ideal diamond chain

In this section we will investigate concurrence (as measure of bipartite entanglement [32, 33]) of the Heisenberg dimers by tracing out the Ising spins in each cluster. We will examine the case of an ideal diamond chain ($J_1 = J_3 \equiv J$, $J_m = 0$). For the construction of eigenvectors of each cluster we will take into account that $\mathcal{H}_k$ possesses a symmetry corresponding to the permutations $\mu_{k_1} \leftrightarrow \mu_{k_2}$ and $\{\mu_{k_2} \leftrightarrow \mu_{k_2}; \mathbf{S}_{k_1} \leftrightarrow \mathbf{S}_{k_2}\}$. Besides, the Hilbert space of the cluster $\mathcal{H}_{cluster}$ can be presented as $\mathcal{H}_{cluster} = \mathcal{H}_{k_1} \otimes \mathcal{H}_{dimer} \otimes \mathcal{H}_{k_2}$, where $\mathcal{H}_{k_1}$, $\mathcal{H}_{dimer}$, $\mathcal{H}_{k_2}$ denotes the Hilbert spaces of μ_{k_1}, Heisneberg dimer and μ_{k_2} respectively. We obtain the following eigenvectors (second and fourth spins are the Heisenberg ones), due to the symmetries and

Hilbert space structure:

$$
\begin{aligned}
|\psi_1\rangle &= \frac{1}{\sqrt{2}}(|\uparrow\uparrow\uparrow\downarrow\rangle + |\uparrow\downarrow\uparrow\uparrow\rangle);\\
|\psi_2\rangle &= \frac{1}{2}(|\uparrow\uparrow\downarrow\downarrow\rangle + |\uparrow\downarrow\downarrow\uparrow\rangle + |\downarrow\uparrow\uparrow\downarrow\rangle + |\downarrow\downarrow\uparrow\uparrow\rangle);\\
|\psi_3\rangle &= \frac{1}{2}(|\uparrow\uparrow\downarrow\downarrow\rangle + |\uparrow\downarrow\downarrow\uparrow\rangle - |\downarrow\uparrow\uparrow\downarrow\rangle - |\downarrow\downarrow\uparrow\uparrow\rangle);\\
|\psi_4\rangle &= \frac{1}{\sqrt{2}}(|\downarrow\uparrow\downarrow\downarrow\rangle + |\downarrow\downarrow\downarrow\uparrow\rangle);\\
|\psi_5\rangle &= \frac{1}{\sqrt{2}}(|\uparrow\uparrow\uparrow\downarrow\rangle - |\uparrow\downarrow\uparrow\uparrow\rangle);\\
|\psi_6\rangle &= \frac{1}{2}(|\uparrow\uparrow\downarrow\downarrow\rangle - |\uparrow\downarrow\downarrow\uparrow\rangle + |\downarrow\uparrow\uparrow\downarrow\rangle - |\downarrow\downarrow\uparrow\uparrow\rangle);\\
|\psi_7\rangle &= \frac{1}{2}(|\uparrow\uparrow\downarrow\downarrow\rangle - |\uparrow\downarrow\downarrow\uparrow\rangle - |\downarrow\uparrow\uparrow\downarrow\rangle + |\downarrow\downarrow\uparrow\uparrow\rangle);\\
|\psi_8\rangle &= \frac{1}{\sqrt{2}}(|\downarrow\uparrow\downarrow\downarrow\rangle - |\downarrow\downarrow\downarrow\uparrow\rangle);\\
|\psi_9\rangle &= |\uparrow\uparrow\uparrow\uparrow\rangle;\\
|\psi_{10}\rangle &= \frac{1}{\sqrt{2}}(|\uparrow\uparrow\downarrow\uparrow\rangle + |\downarrow\uparrow\uparrow\uparrow\rangle);\\
|\psi_{11}\rangle &= \frac{1}{\sqrt{2}}(|\uparrow\uparrow\downarrow\uparrow\rangle - |\downarrow\uparrow\uparrow\uparrow\rangle);\\
|\psi_{12}\rangle &= |\downarrow\uparrow\downarrow\uparrow\rangle;\\
|\psi_{13}\rangle &= |\uparrow\downarrow\uparrow\downarrow\rangle;\\
|\psi_{14}\rangle &= \frac{1}{\sqrt{2}}(|\uparrow\downarrow\downarrow\downarrow\rangle + |\downarrow\downarrow\uparrow\downarrow\rangle);\\
|\psi_{15}\rangle &= \frac{1}{\sqrt{2}}(|\uparrow\downarrow\downarrow\downarrow\rangle - |\downarrow\downarrow\uparrow\downarrow\rangle);\\
|\psi_{16}\rangle &= |\downarrow\downarrow\downarrow\downarrow\rangle;
\end{aligned}
\tag{2}
$$

and the corresponding eigenvalues:

$$
\begin{aligned}
&E_1 = \frac{1}{4}\left(-2H + J_2\right); E_2 = E_3 = \frac{J_2}{4}; E_4 = \frac{1}{4}(J_2 + 2H);\\
&E_5 = \frac{1}{4}(-2H - 3J_2); E_6 = E_7 = -\frac{3J_2}{4}; E_8 = \frac{1}{4}(2H - 3J_2);\\
&E_9 = -\frac{3H}{2} + \frac{J_2}{4} + J; E_{10} = E_{11} = -H + \frac{J_2}{4}; E_{12} = -\frac{H}{2} + \frac{1}{4}\left(J_2 - 4J\right);\\
&E_{13} = \frac{H}{2} + \frac{1}{4}\left(J_2 - 4J\right); E_{14} = E_{15} = \frac{1}{4}(J_2 + 4H); E_{16} = \frac{3H}{2} + \frac{J_2}{4} + J.
\end{aligned}
\tag{3}
$$

We study *concurrence* $C(\rho)$, to quantify pairwise entanglement [32,33], defined as

$$C(\rho) = max\{\lambda_1 - \lambda_2 - \lambda_3 - \lambda_4, 0\}, \tag{4}$$

where λ_i's are the square roots of the eigenvalues of the corresponding operator for the density matrix

$$\tilde{\rho} = \rho_{12}(\sigma_1^y \otimes \sigma_2^y)\rho_{12}^*(\sigma_1^y \otimes \sigma_2^y) \tag{5}$$

in descending order. Since we consider pairwise entanglement, we should use the reduced density matrix ρ_{12}, by tracing out two Ising spins of the cluster. It is obvious that the only entangled pair is formed by the Heisenberg spins. Other pairs are disentangled (separable) because of the classical (diagonal) character of the Ising-type interaction between them. Hence we will be interested in the reduced density matrix, constructed by tracing out two Ising-type spins μ_{k_1} and μ_{k_2}, i.e. $\rho_{12} = \mathrm{Tr}_{\{\mu_{k_1},\mu_{k_2}\}}\rho$ and the full density matrix ρ is defined as (here and further Boltzmann constant is set to be $k_B = 1$)

$$\rho = \frac{1}{Z}\sum_{k=1}^{16}\exp(-E_k/T)|\psi_k\rangle\langle\psi_k|, \tag{6}$$

where Z is the partition function ($Z = \mathrm{Tr}\rho$), $|\psi_k\rangle$ and E_k should be taken from equations (2) and (3) respectively. Here we skip the specific details and provide the result of the final calculations of the concurrence for a reduced density matrix ρ_{12}, taking into account that the Hamiltonian $\mathcal{H}_k$ is translationary invariant with a symmetry $[S_z, \mathcal{H}_k] = 0$ ($S_z = 1/2(\mu^z_{k_1} + \mu^z_{k_2}) + S^z_{k_1} + S^z_{k_2}$) [34–36]:

$$C(\rho) = \frac{2}{Z}max(|y| - \sqrt{uv}, 0), \tag{7}$$

where

$$\begin{aligned}
u = &\quad e^{-\frac{-2H+4J+J_2}{4T}}\left(e^{\frac{H}{2T}} + e^{J/T}\right)^2,\\
v = &\quad e^{-\frac{6H+4J+J_2}{4T}}\left(e^{\frac{H+2J}{2T}} + 1\right)^2,\\
w = &\quad \frac{1}{2}\left(e^{\frac{H}{2T}} + 1\right)^2\left(e^{\frac{J_2}{T}} + 1\right)e^{-\frac{2H+J_2}{4T}},\\
y = &\quad \frac{1}{2}\left(e^{\frac{H}{2T}} + 1\right)^2\left(e^{\frac{J_2}{T}} - 1\right)e^{-\frac{2H+J_2}{4T}},\\
Z = &\quad e^{-\frac{6H+4J+J_2}{4T}}\left(e^{\frac{H+J}{T}} + e^{\frac{2(H+J)}{T}} + e^{\frac{2H+J}{T}} + 2e^{\frac{H+2J}{2T}} + \right.\\
&\quad e^{\frac{H+2J}{T}} + 2e^{\frac{3H+2J}{2T}} + 2e^{\frac{5H+2J}{2T}} + e^{\frac{H+J+J_2}{T}} + e^{\frac{2H+J+J_2}{T}} +\\
&\quad \left.2e^{\frac{3H+2J+2J_2}{2T}} + e^{\frac{3H}{T}} + 1\right).
\end{aligned} \tag{8}$$

In equation (2), one finds a set of states with maximum value of entanglement, for which the Heisenberg dimer is in singlet or triplet state ($|\psi_i\rangle$'s with $i = 1, ..., 8$). As for the rest of the states ($|\psi_i\rangle$'s with $i = 9, ..., 16$) the Heisenberg dimer is in separable state and therefore these $|\psi_i\rangle$'s are non-entangled ones.

3.1. Zero field effects

We start with the investigation of the behavior of $C(\rho)$ at zero magnetic field ($H = 0$). We will discuss here three regimes, depending on the value of $J-J_2$: $J-J_2 > 0$, $J-J_2 < 0$ and $J-J_2 = 0$. In the first case, as one finds from (3), that the ground state contains two-fold degenerate states $|\psi_{12}\rangle$ and $|\psi_{13}\rangle$. Since these states are factorable, the corresponding dependency curve of $C(\rho)$ from temperature T starts from $C(\rho) = 0$ (figure 2). Furthermore, the entanglement can be invoked by increasing the temperature (for values of $J - J_2$ close to 0). This happens since the contribution of entangled states in the mixture ρ increases with growth of temperature T. The local maximum, appearing here arises due to the optimal thermal mixing of all eigenstates in the system. This maximum becomes narrower and smaller and gradually vanishes by increasing $J - J_2$. But the value of $J - J_2$ corresponding to disappearing of $C(\rho)$ also depends on the value

of J_2 (e.g. for $J_2 = 1$, $J - J_2 \approx 0.2$). The latter becomes obvious, if one takes into account that J_2, being the coupling constant of the Heisenberg type interaction between dimeric units, is responsible for the strength of quantum correlations between Heisenberg spins. We would like to emphasize here that in the case $J - J_2 > 0$ the system exhibits weak ($0 < J_2 < J$) or no frustration ($J_2 < 0$).

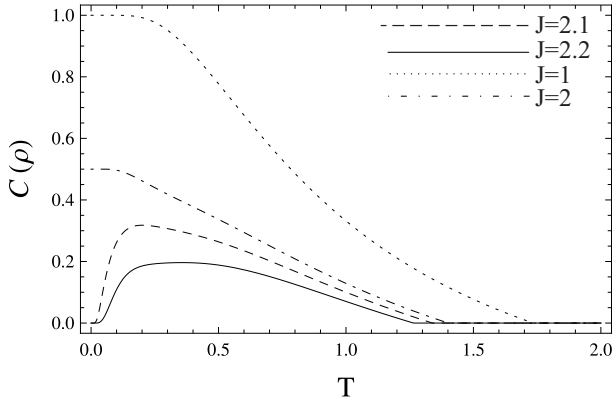

Figure 2. Concurrence $C(\rho)$ versus temperature T for $J_2 = 2$, $J_m = 0$, $H = 0$, and different values of $J_1 = J_3 \equiv J$.

In the second case, when $J - J_2 < 0$, the system will obviously manifest more of its quantum nature. Firstly, the dependency curve of $C(\rho)$ on temperature starts from $C(\rho) = 1$ at $T = 0$ (figure 2), which is the consequence of the fact that at zero temperature the maximum entangled states $|\psi_5\rangle$, $|\psi_6\rangle$, $|\psi_7\rangle$ and $|\psi_8\rangle$ form four-fold degenerate ground state with the value of $C(\rho) = 1$ for the corresponding reduced density matrix ρ_{12}. When the temperature is increased, the concurrence gradually disappears because of the thermal mixing with other states of the system (including the factorable ones). The critical temperature T_c, corresponding to the dying out of quantum correlations in the system can be found form the equation $C(\rho) = 0$. It has the following form:

$$x^{-J}\left(x^J + 1\right)^2 = 2\left|x^{J_2} - 1\right|, \tag{9}$$

where $x = e^{1/T}$. The solution can be presented in the form $T_c = J/\log a$ (when $J - J_2 < 0$), where a depends on the ratio parameter J_2/J. Increasing this ratio, a decreases, but the linear dependence on J remains (e.g. when $J_2/J = 2$, $a = \frac{1}{4}(3 + \sqrt{17})$).

Finally, the case $J - J_2 = 0$ can be regarded as a boundary case in the following sense. Here the ground state is six-fold degenerate, containing additionally $|\psi_{12}\rangle$ and $|\psi_{13}\rangle$, besides $|\psi_5\rangle$, $|\psi_6\rangle$, $|\psi_7\rangle$ and $|\psi_8\rangle$ (in other words all the states as in previous two cases). Since the $|\psi_{12}\rangle$ and $|\psi_{13}\rangle$ are factorable, this leads to lower entanglement of the ground state's reduced matrix, that is $C(\rho) = 1/3$ (figure 2). Moreover, the discussed above critical temperature T_c is lower, than in the case $J - J_2 < 0$ (although again $T_c = J/\log a$ with $a = 2 + \sqrt{5}$).

On the other hand, as it can be seen from figure 2, there are two critical temperatures in the case $J - J_2 > 0$ (corresponding to arising and vanishing of entanglement) [37]. The dependence of T_c on the ratio parameter J_2/J is shown in figure 3. In the area $0 < J_2/J < 1$, there are two critical temperatures (as mentioned above), while for the values $J_2/J \geq 1$, the dependence is a linear one.

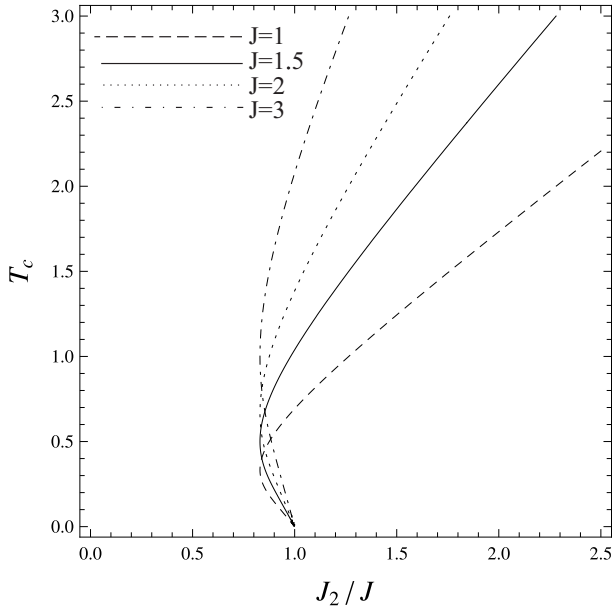

Figure 3. Critical temperature T_c corresponding to the vanishing or arising of entanglement at zero magnetic H versus ration parameter J_2/J for different values of $J_1 = J_3 \equiv J$.

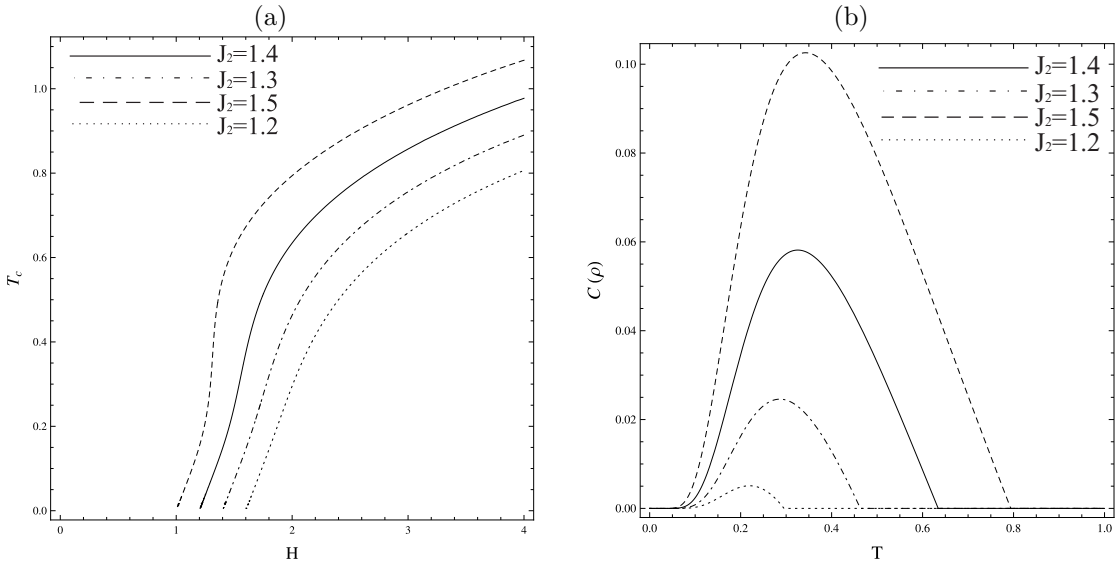

Figure 4. (a) Critical temperature T_c corresponding to the vanishing or arising of entanglement versus magnetic field H for $J_1 = J_3 \equiv J = 2$ and different values of J_2; (b) Concurrence $C(\rho)$ versus temperature T for $J_1 = J_3 \equiv J = 2$ and different values of J_2.

3.2. Incorporation of magnetic field

In this subsection we concentrate on the effects driven by magnetic field. Firstly we will discuss how the magnetic field affects the introduced above critical temperature T_c. While increasing H, T_c increases too, but it always remains lower than $J_2/\log 3$ (in other words $\lim_{H\to\infty} T_c = J_2/\log 3$). However, when $T \to 0$, $C(\rho)$ remains finite and becomes zero only at absolute zero temperature $T = 0$. In other words in the area of low temperatures the behavior of concurrence is smooth, in contrast with the case when magnetic field is absent.

Now, we concentrate on the dependence of $C(\rho)$ on magnetic field. Because of the above

introduced ground state structure of the system the dependency curve of $C(\rho)$ from magnetic field at zero temperature has a dip at $H = 0$, corresponding to $C(\rho) = 1/3$, when $J - J_2 = 0$ and has no dip, when $J - J_2 < 0$ (figure 5). When Ising-type interaction is stronger than the Heisenberg one ($J - J_2 > 0$), there is no magnetic entanglement [23] in the system (at zero temperature). Furthermore, magnetic entanglement is of a higher value than that at zero magnetic field in the case $J - J_2 = 0$, due to the fact that ground state here is two-fold degenerate and contains $|\psi_5\rangle$ and $|\psi_{12}\rangle$ with the value $C(\rho) = 1/2$ for the corresponding reduced density matrix. $C(\rho)$ becomes zero for the case $J - J_2 \leq 0$ at the values of H, corresponding to saturation field, that is when the non-entangled state $|\uparrow\uparrow\uparrow\uparrow\rangle$ (in the area $H > 0$) or $|\downarrow\downarrow\downarrow\downarrow\rangle$ (in the area $H < 0$) becomes a ground state. One can find the described values of H from the conditions $E_9 = E_5$ and $E_{16} = E_8$, giving $H_s^+ = J + J_2$ and $H_s^- = -J - J_2$, respectively. Thermal effects smoothes the step-like behavior of concurrence in the case when $J - J_2 \geq 0$ and induces thermal entanglement when $J - J_2 > 0$ (see figure 2). The further increasing of the temperature causes the quantum correlations' eventually dying out for both cases.

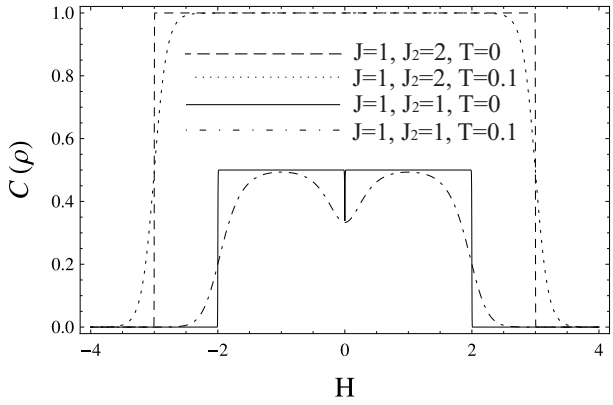

Figure 5. Concurrence $C(\rho)$ versus magnetic field H for different values of temperature, J_2 and $J_1 = J_3 \equiv J$.

Summarizing, in figure 6 we also plot three-dimensional dependencies of the concurrence $C(\rho)$ versus temperature T and magnetic field H.

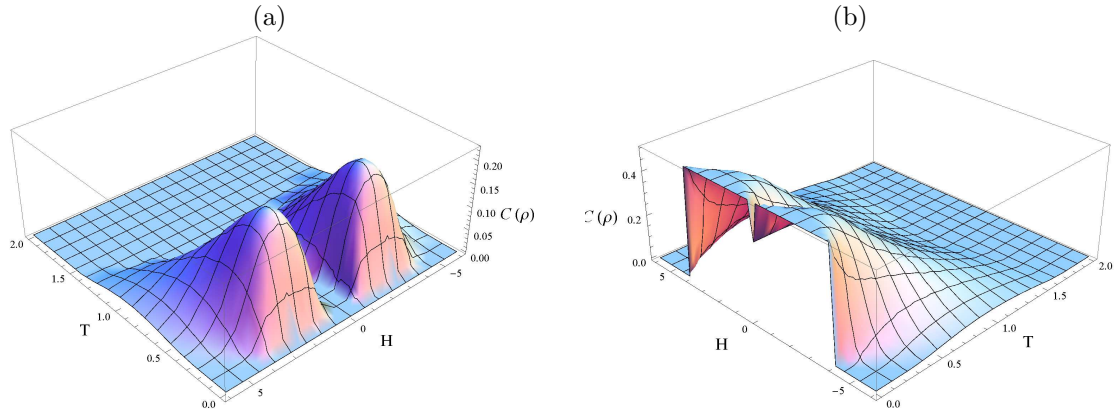

Figure 6. Concurrence $C(\rho)$ versus magnetic field H and temperature T for (a) $J_2 = 1.7$ and $J_1 = J_3 \equiv J = 2$; (b) $J_2 = 2$ and $J_1 = J_3 \equiv J = 2$.

4. Conclusion

In this paper we have studied the thermal entanglement of spin-1/2 Ising-Heisenberg model on an ideal diamond chain, which has been proposed to understand a frustrated magnetism

of the series of compounds, like $A_3Cu_3(PO_4)_4$ with A=Ca, Sr, $Bi_4Cu_3V_2O_{14}$, $Cu_3(TeO_3)_2Br_2$ and $Cu_3(CO_3)_2(OH)_2$. Considering that diamond chain structure describes a broad class of materials (within different values of exchange interaction parameters) and that the exact value of coupling constants for azurite ($Cu_3(CO_3)_2(OH)_2$) is still under scrutinizing question, we have studied the phase structure and entanglement properties of the system in a wide range of Ising-type interaction constants $J_1 = J_3 \equiv J$ and Heisenberg-type J_2. Taking into account the classical and hence separable character of Ising-type interactions which are coupling adjacent Heisenberg dimers, we have calculated the entanglement of each of these dimers separately. We have used the concurrence for quantifying the amount of entanglement between two Heisenberg-type spins, by tracing out Ising-type ones from the density matrix of the diamond-shaped cluster (the only entangled pair here is the Heisenberg dimer). The incorporation of external magnetic field has been also invoked.

We have revealed a number of regimes with distinct ground state structure and qualitatively different thermodynamic behavior, depending on the relations between J and J_2 and values of magnetic field H. We found that in general for a dominant Heisenberg-type interaction ($J_2 > J$) the system's ground state is maximally entangled, but increasing the temperature, pure quantum correlations eventually disappear. On the other hand, for a dominant Ising-type interaction ($J > J_2$) the ground-state is non-entangled, whether the temperature gives rise to thermal entanglement. In other words the presence of competing interactions in the system and geometrical structure of the chain, each leading to a frustration, makes the phase structure of the system rich and gives rise to an interesting physical behavior. Finally, the adopted model guaranties experimental realization for suitable theoretical treatment and our results will be useful for further experimental detection of entanglement in the diamond chain structured macroscopic samples by means of entanglement witnesses (e.g. built from measurements of magnetic susceptibility [38]).

Acknowledgments

The work was supported by ECSP-09-08-SASP NFSAT, PS-2497 ANSEF grants. The work of C. B. was supported in part by the GACR-P201/10/1509 grant and by the research plan MSM6840770039.

References

[1] Vedmedenko E Y, Udvardi L, Weinberger P, Wiesendanger R 2007 *Phys. Rev.* B **75** 104431
[2] Diep H T, Ed. 2004 *Frustrated Spin Sysytems* (Singapore: World Sceintific)
[3] Gardner J S, Gingras M J P, Greedan J E 2010 *Rev. Mod. Phys* **82** 53
[4] Ananikian N S, Avakian A R, and Izmailian N Sh 1991 *Physica* A **172** 391
[5] Zhitomirsky M E, Honecker A, Petrenko O A 2000 *Phys. Rev. Lett.* **85** 3269
[6] Kikuchi H *et al* 2005 *Phys. Rev. Lett.* **94** 227201
[7] Valverde S, Rojas O and Souza de S M 2008 *J. Phys.: Condens. Matter* **20** 345208
[8] Li Y-Ch, Li S-S 2008 *Phys. Rev.* B **78** 184412
[9] Rule K C *et al* 2008 *Phys. Rev. Lett.* **100** 117202
[10] Aimo F, Kramer S, Klanjsek M, Horvatic M, Berthier C 2011 *Phys. Rev.* B **84** 012401
[11] Takano K, Kubo K, and Sakamoto H 1996 *J. Phys.: Condens. Matter* **8** 6405
[12] Tonegawa T, Okamoto K, Hikihara T, Takahashi Y and Kaburagi M 2001 *J. Phys. Chem. Solids* **62** 125
[13] Tonegawa T, Okamoto K, Hikihara T, Takahashi Y and Kaburagi M 2000 *J. Phys. Soc. Japan* **69** (suppl. A) 332
[14] Honecker A and Lauchli A 2001 *Phys. Rev.* B **63**, 174407
[15] Jeschke H *et al* 2011 *Phys. Rev. Lett.* **106** 217201
[16] Uematsu D, Sato M 2007 *J. Phys. Soc. Japan* **76**, 084712
[17] Drillon M, Belaiche M, Legoll P, Aride J, Boukhari A, Moqine A 1993 *J. Magn. Magn. Mater.* **128** 83
[18] Sakurai H *et al* 2002 *J. Phys. Soc. Japan* **71** 1161
[19] Rojas O, Souza de S M, Ohanyan V, Khurshudyan M 2011 *Phys. Rev.* B **83** 094430
[20] Valverde J S, Rojas O, Sousa de S M 2008 *J. Phys.: Condens. Matter* **20** 345208

[21] Amico L, Fazio R, Osterloh A, Vedral V 2008 *Rev. Mod. Phys.* **80** 517
[22] Gühne O, Toth G 2009 *Phys. Reports* **474** 1
[23] Arnesen M C, Bose S, and Vedral V 2001 *Phys. Rev. Lett.* **87** 017901
[24] Gunlycke D, Kendon V M, Vedral V, and Bose S 2001 *Phys. Rev.* A **64** 042302
[25] Ananikian N S, Ananikyan L N, Chakhmakhchyan L A, Kocharian A N 2011 *J. Phys. A: Math. Gen.* **44** 025001
[26] Abgaryan V S, Ananikian N S, Ananikyan L N and Kocharian A N 2011 *Phys. Scr.* **83** 055702
[27] Ananikian N, Ananikyan L, Lazaryan H 2011 *Physics of Atomic Nuclei*, in press (*Preprint* cond-mat/1102.2603v2)
[28] Larsson D and Johannesson H 2005 *Phys. Rev. Lett.* **95** 196406
[29] Alba V, Tagliacozzo L, and Calabrese P 2010 *Phys. Rev.* B **81** 060411(R)
[30] Souza A M, Soares-Pinto D O, Sarthour R S, Oliveira I S, Reis M S, Brandao P, and Santos dos A M 2009 *Phys. Rev.* B **79** 054408
[31] Soares-Pinto D O, Souza A M, Sarthour R S, Oliveira I S, Reis M S, Brandao P, and Santos dos A M 2009 *Eur. Phys. Lett.* **87** 40008
[32] Hill S and Wootters W K 1997 *Phys. Rev. Lett.* **78** 5022
[33] Wootters W K 1998 *Phys. Rev. Lett.* **80** 2245
[34] Rau A R P 2009 *J. Phys. A: Math. Gen.* **42** 412002
[35] Rau A R P, Ali M, Alber G 2008 *Eur. Phys. Lett.* **82** 40002
[36] Yu T and Eberly J H 2006 *Phys. Rev. Lett.* **97** 140403
[37] Wang X, Fu H, Solomon A I 2001 *J. Phys. A: Math. Gen.* **34** 11307
[38] Wiesniak M, Vedral V, and Brukner C 2005 Magnetic susceptibility as a macroscopic entanglement witness *New J. Phys.* **7** 258